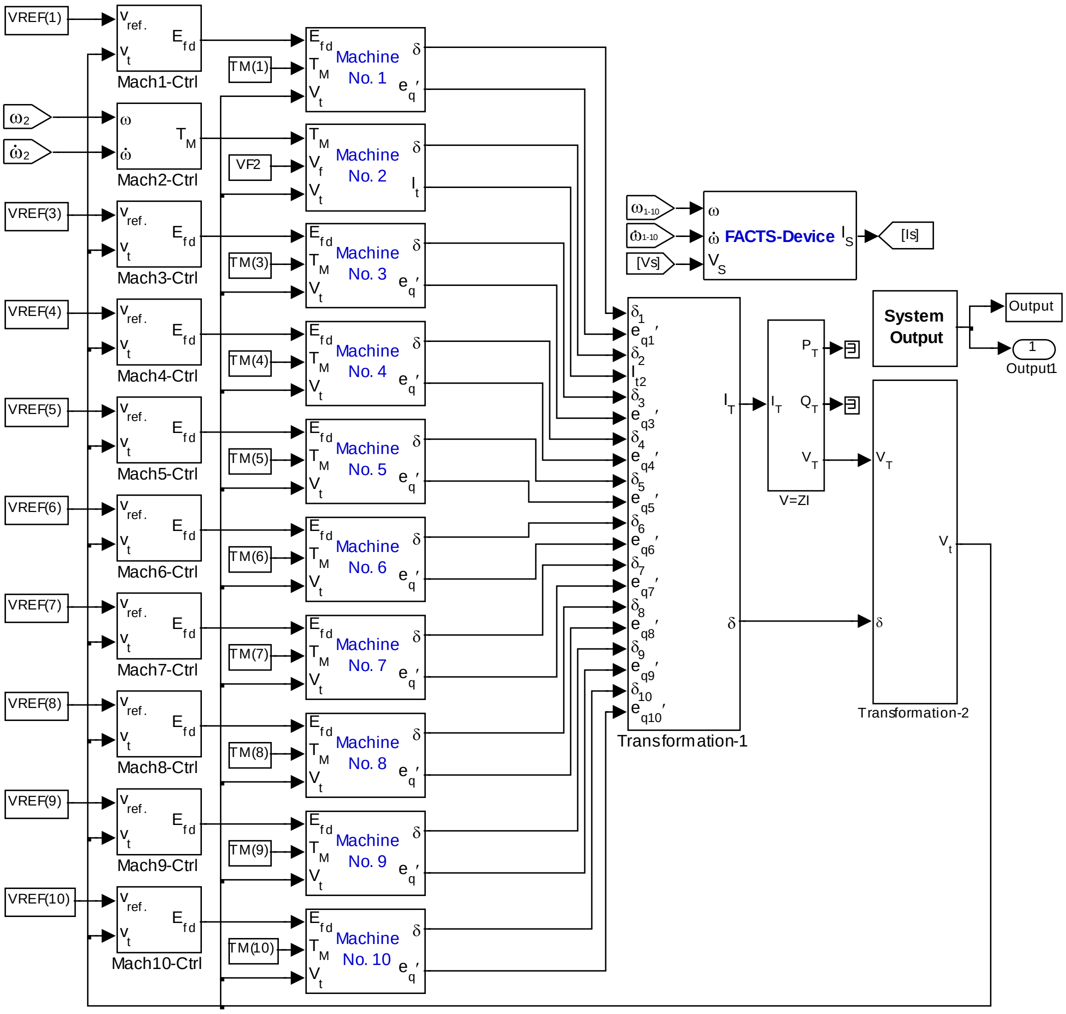

Fig.11 The SIMULINK model of the multi-machine power system

$$\left.\begin{aligned} H_c(s) &= K_{pc} + \frac{K_{ic}}{S} + K_{dc}S \\ H_\phi(s) &= K_{p\phi} + \frac{K_{i\phi}}{S} + K_{d\phi}S \end{aligned}\right\} \qquad (18)$$

5. Digital Simulation

The SIMULINK model of a multi-machine power system including a SVC/STATCOM is shown in Fig.11. The differential equations describe each generator model are represented by separate blocks. The FACTS-device is also represented by a single block that describes its dynamic behavior. FACTS-device's sub-system and generators' sub-systems are linked together through the block that represents the electrical network to configure the whole system. The system initial load flow calculation is computed by a m-file that accepts all system data and returns the system initial conditions. The loads have been replaced with a constant impedance-type model. The system model is tested before applying the disturbance for a certain period (200 ms) then it is subjected to a disturbance and tested for 5 s using numerical integration technique.

5.1 Optimal Location of FACTS-devices

FACTS-devices are placed at a suitable bus to enhance the power system stability and to improve the damping characteristics of the power system. The system performance index technique is applied to choose the optimal location. The power system transient performance is obtained when it is subjected to a 3-phase short circuit. Fig.12 shows the values of performance index for different buses location when the SVC is equipped with PID controller with feedback signal of the speed deviations for all generators. According to the values of performance index, the optimal location for the SVC is at bus 28. Also, Fig.13 shows the values of performance index for different buses location when the STATCOM is attached to the system. This figure results in, the optimal location is bus No. 30.

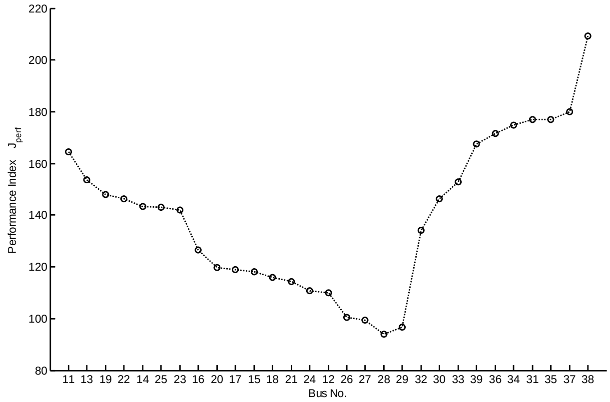

Fig.12 The system's performance index versus the SVC location

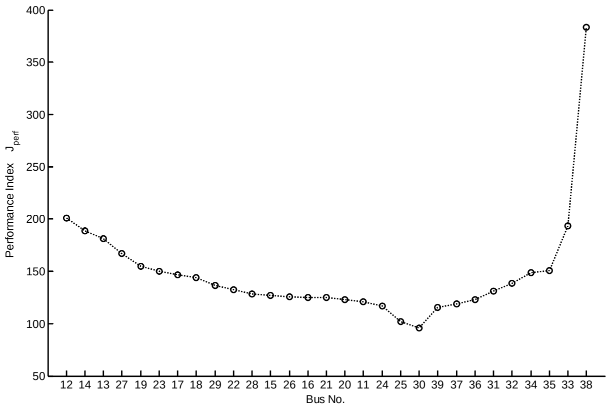

Fig.13 The system's performance index versus the STATCOM location

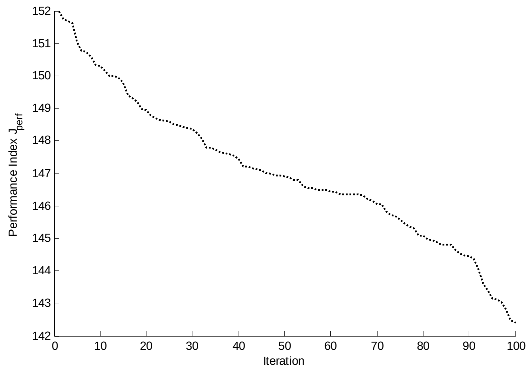

Fig.14 The system performance versus the iteration in case of SVC

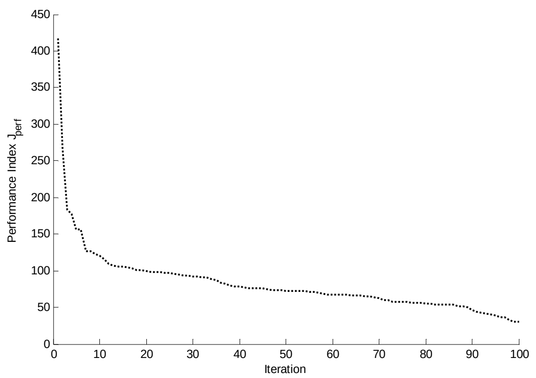

Fig.15 The system performance versus the iteration in case of STATCOM

5.2 FACTS-devices controller parameters

After choosing the best location for the SVC/STATCOM, with the MATLAB optimization toolbox the control systems parameters of the FACTS-devices are determined by minimizing the system performance (J_{perf}), which is given by:

$$J_{perf} = \int_0^\infty e(t)*t^2 \qquad (19)$$

where, e(t) =Σ{All of the system output deviations. Such as speed, rotor angle, valve position, etc.}, t: is the time.

The system performance versus the iteration of the optimization is shown in Fig.14 for the case of SVC. And Fig.15 shows the case of attaching the STATCOM. With the help of MATLAB optimization toolbox the parameters of the SVC/STATCOM PID controllers are given in Appendix-A.

6. Simulation Results

The time response of the studied multi-machine power system involving a SVC/STATCOM is illustrated when it is subjected to different disturbances. The FACTS-based stabilizers' parameters are optimally designed when coordinated with the power system controllers with fixed parameters by the help of MATLAB optimization techniques.

The generators' rotor angles and the SCG valve position are used to evaluate the effectiveness of the proposed nonlinear model-based optimization process. The simulation results are obtained in a comparative form to show the effectiveness of FACTS-devices on the system performance.

Fig.16 shows the response when the system is subjected to a 3-phase short circuit at F_1. This figure illustrates that, SVC positively affects the system's performance and adds more damping to it. For Fig.17, the comparison is focused on the effect of FACTS-devices only. The figure shows that, the system's response with STATCOM is more damped. So, all system variables return to their initial values quickly in case of STATCOM compared with SVC. Fig.18 through Fig.20 show the dynamic response of the system such as load increase, one line outage, or disconnection of a transformer. these results confirm the ability of STATCOM to increase the system's damping.

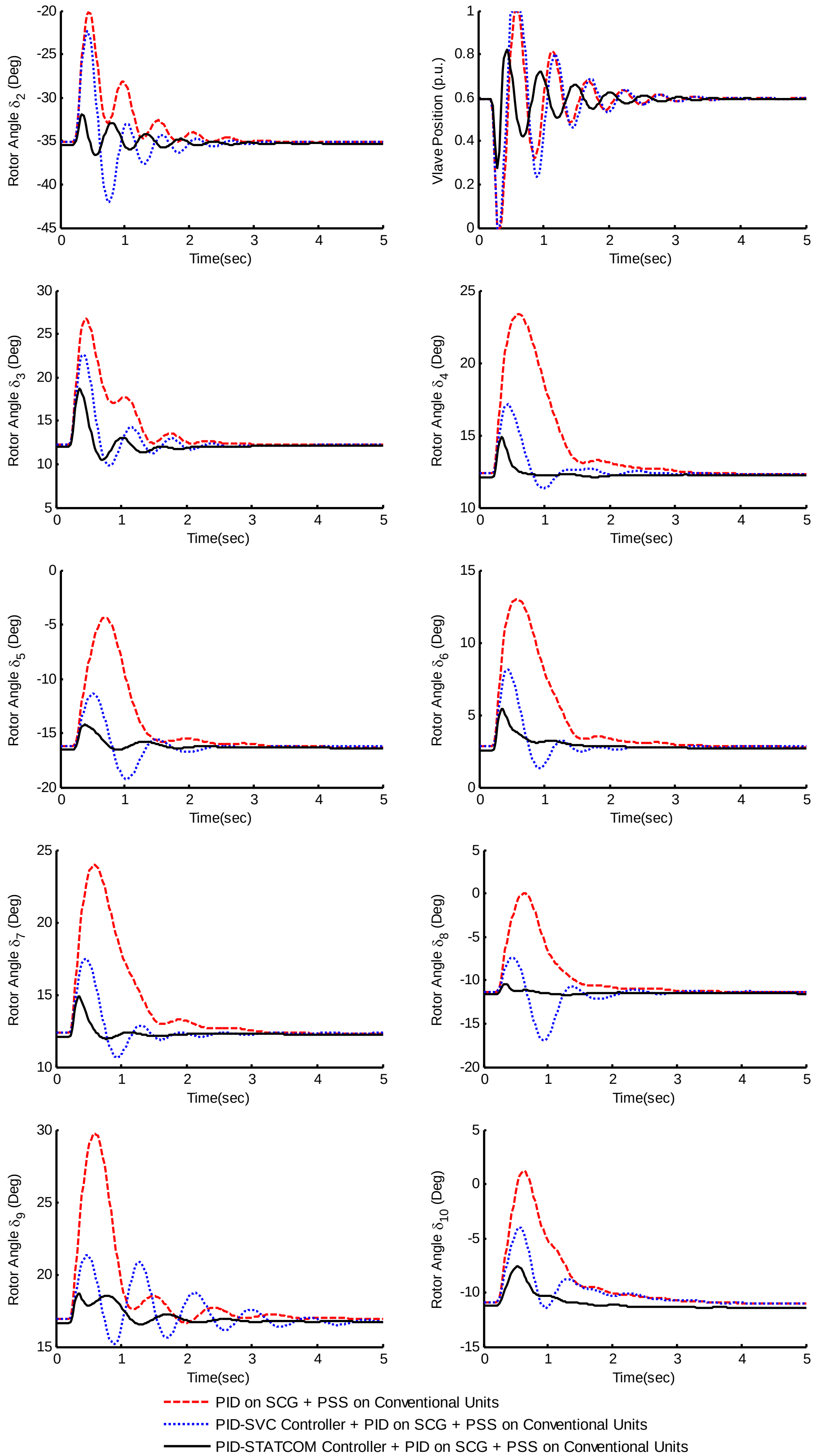

Fig.16 System transient response to a 3-phase short circuit for a 100 ms at F_1

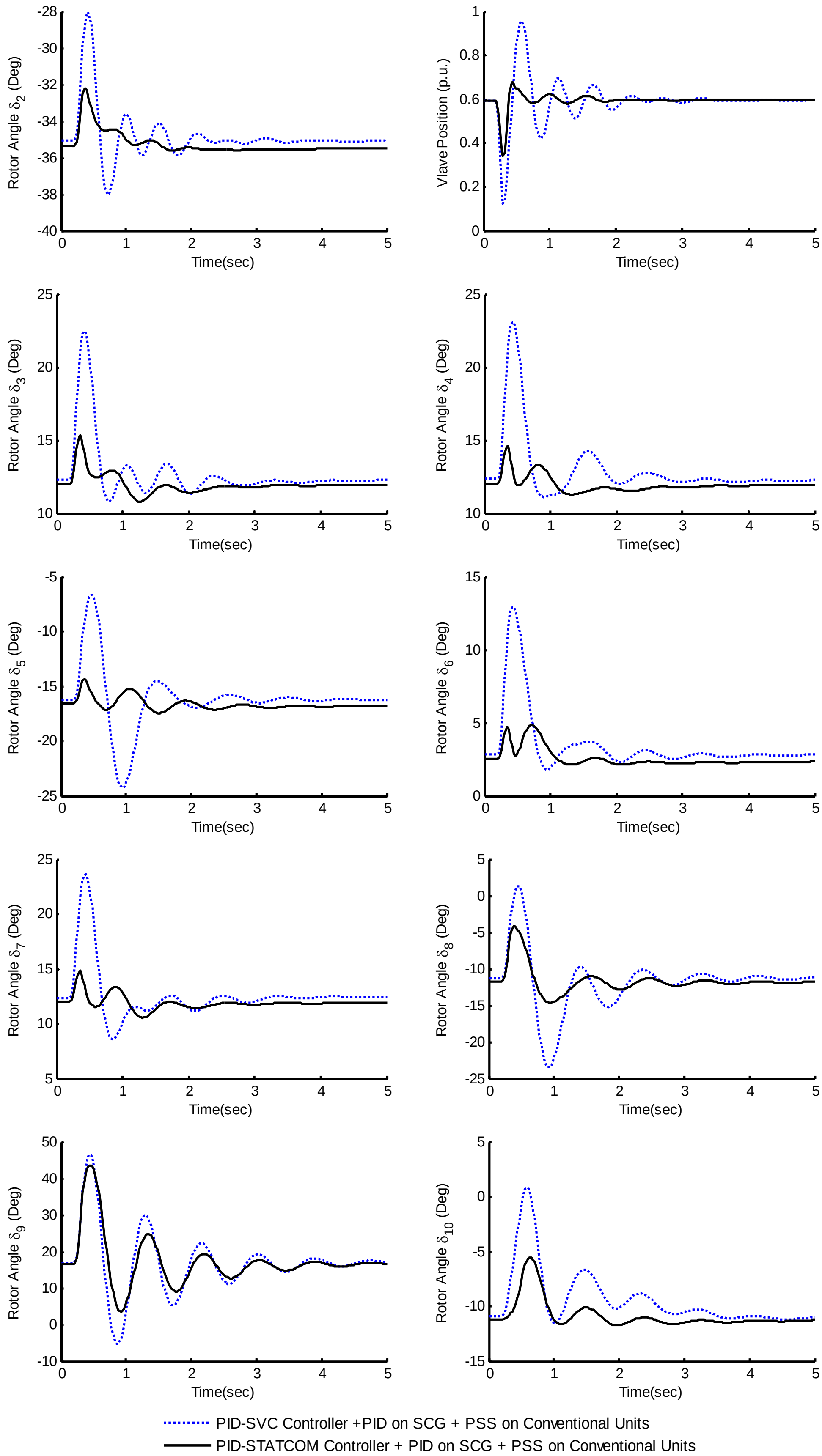

Fig.17 System transient response to a 3-phase short circuit for a 100 ms at F_2

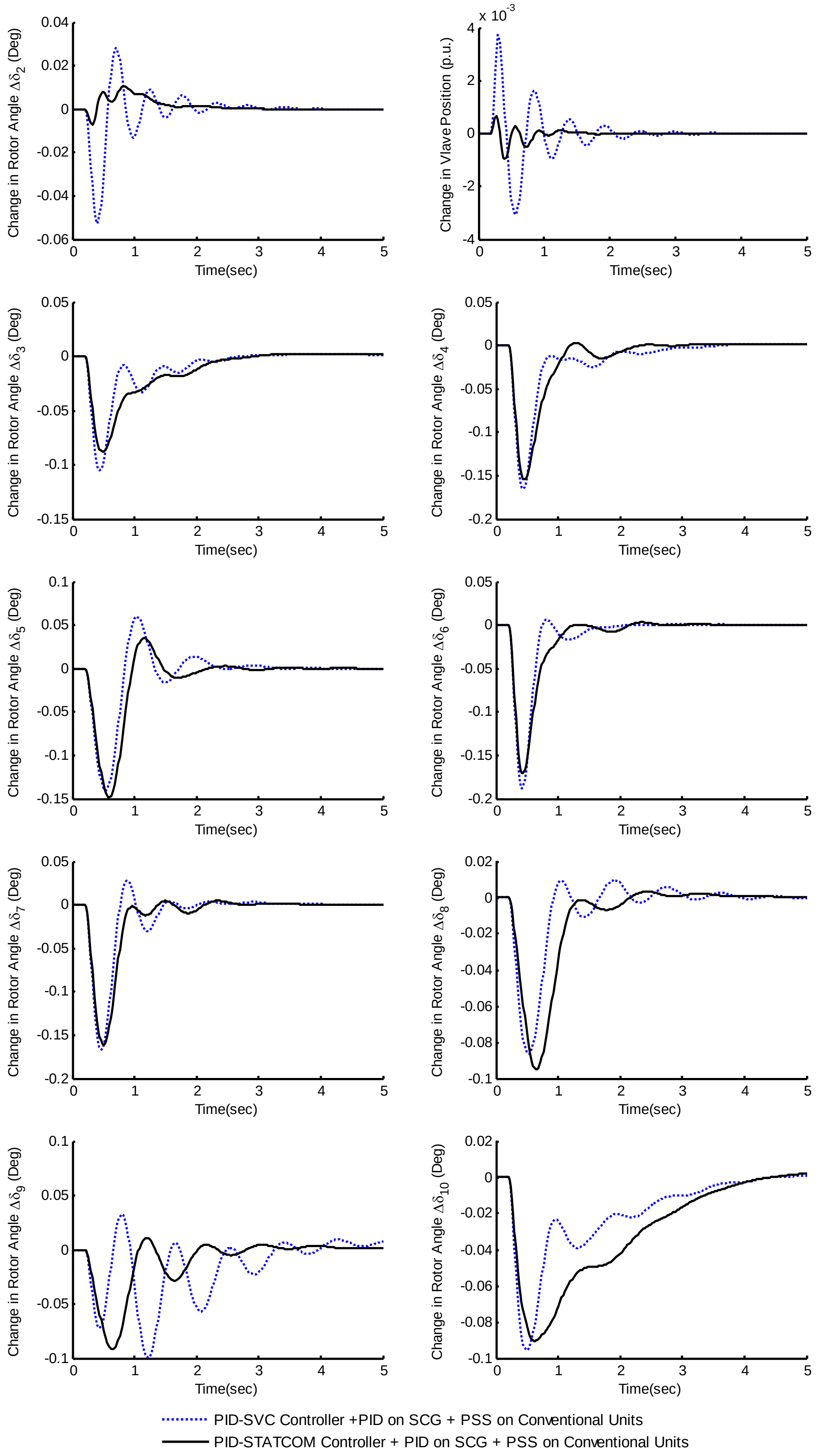

Fig.18 Dynamic response to a 10% load increase at bus 16 for 100 ms

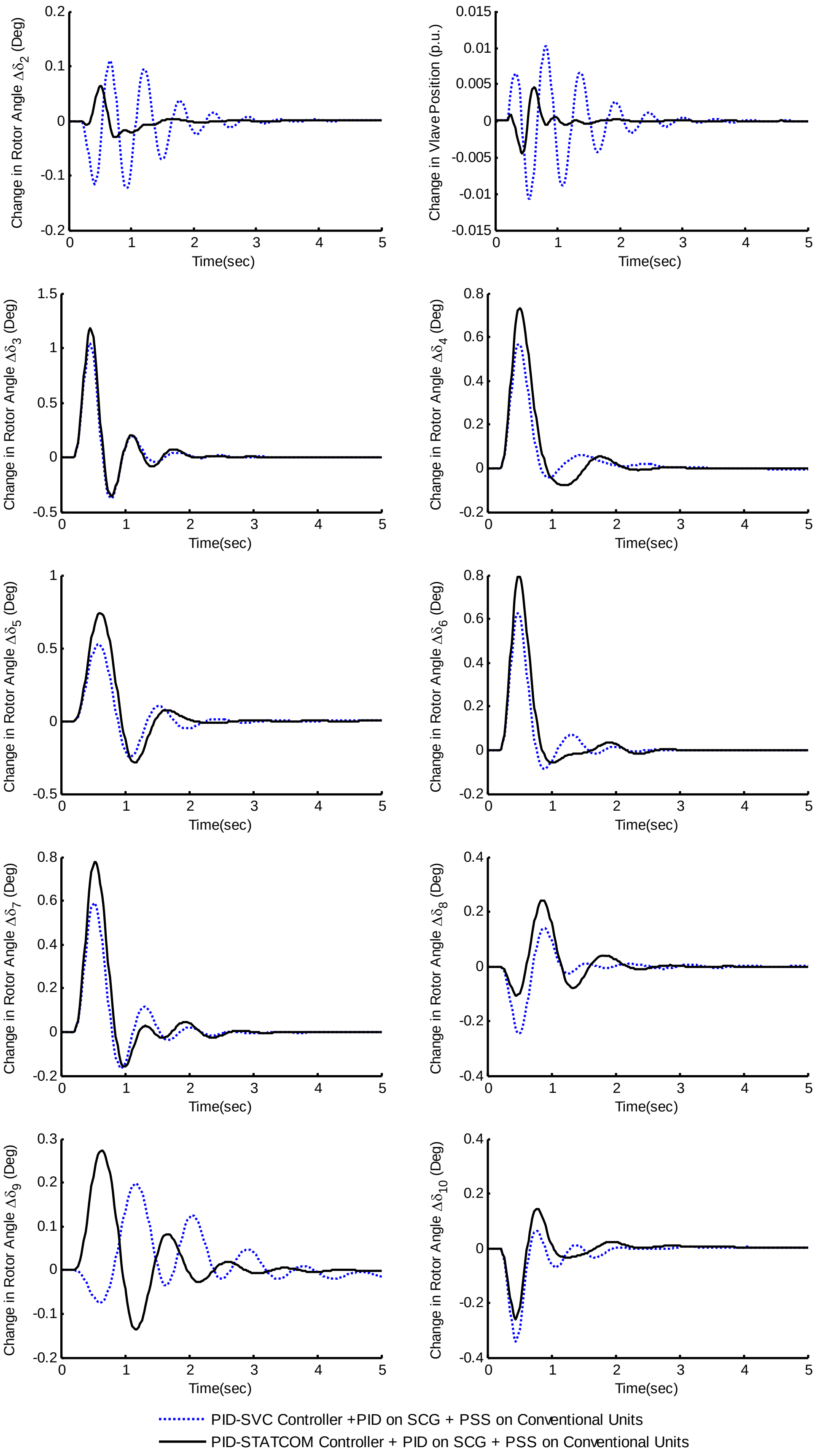

Fig.19 Dynamic response to one line outage (14-33) for 200 ms

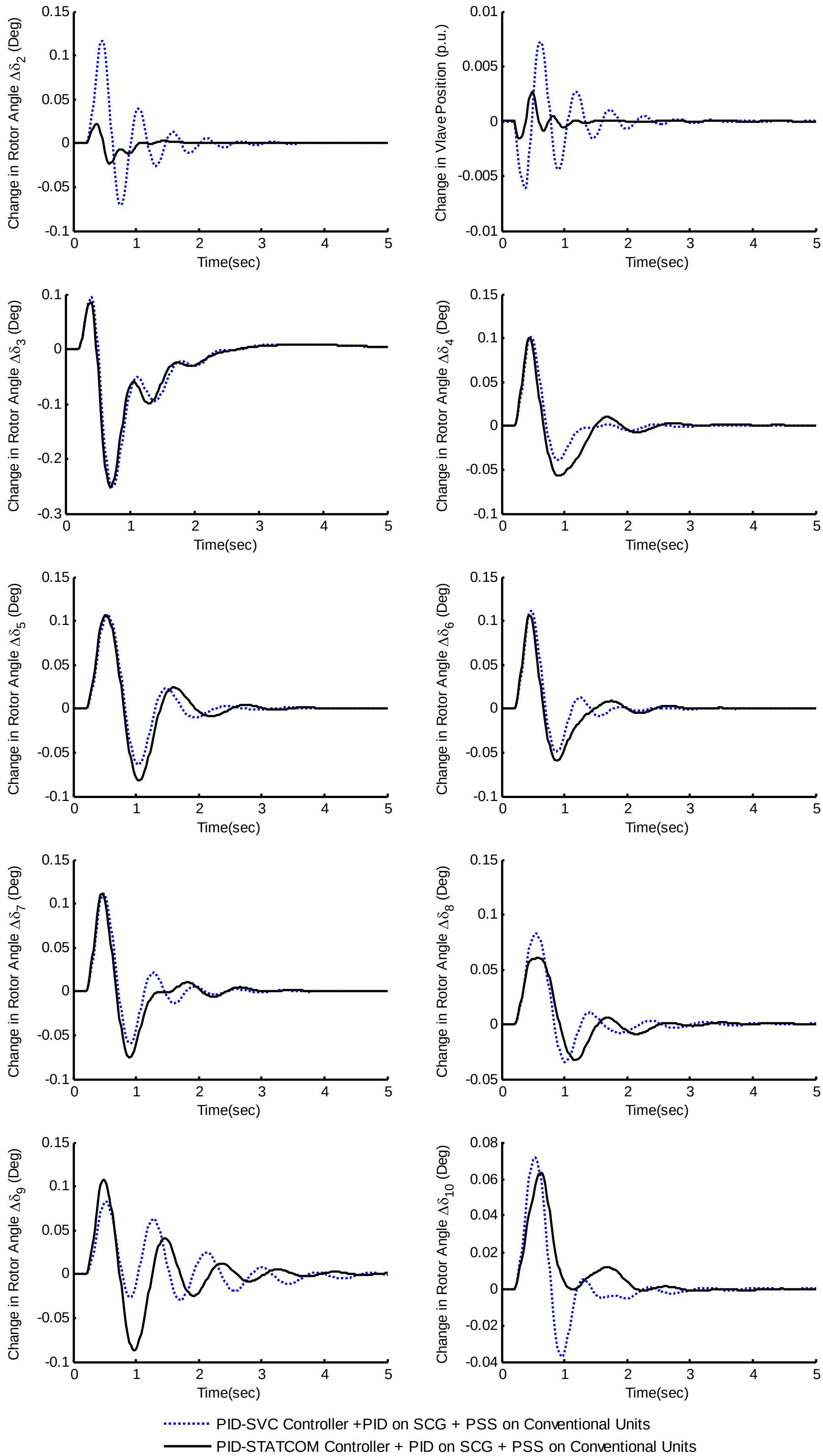

Fig.20 Dynamic response to a disconnection of transformer (11-12) for 200 ms

7. CONCLUSIONS

The paper presents FACTS stabilizers based PID controllers as a approach to improve the performance of SCGs in multi-machines power systems. Conventional generating units are equipped with excitation control systems. While, SCG is equipped with PID controller, designed using pole placement technique, in its governor loop. The FACTS-device are equipped with PID controllers designed using the system performance minimization. The simulation results, show the effectiveness of the STATOM-based controller over the SVC-based controller for various disturbances in terms of damping increase, system variables fast return to their nominal values and less movements of the SCG governor valve.

8. APPENDICES

Appendix-A

SCG parameters:

2000 MVA, 1700 MW, 3000 rpm
$X_d=X_q=0.5457$ p.u.
$X_{D1}=X_{Q1}=0.2567$ p.u.
$X_{D2}=X_{Q2}=0.4225$ p.u., $X_f=0.541$ p.u.
$X_{fd}=X_{fD1}=X_{dD1}=X_{dD2}=X_{D1D2}=0.237$ p.u.
$X_{qQ1}=X_{qQ2}=X_{Q1Q2}=0.237$ p.u., $X_{fD2}=0.3898$ p.u.
$R_a=0.003$ p.u., $R_{D1}=R_{Q1}=0.1008$ p.u.
$R_{D2}=R_{Q2}=0.00134$ p.u.
Field time constant=750 s
H=3 KW.s/KVA

Turbines and governor system parameters

$T_{HP}= T_{GM}=0.1$ s, $F_{HP}=26\%$, $T_{IP}=0.1$ s, $F_{IP}=42\%$
$T_{LP}=0.3$ s, $F_{LP}=32\%$, $T_{HR}=10$ s, $P_o=1.2$ p.u.

SVC parameters

$R_{trans}=0.01$ p.u., $X_{trans}=0.145$ p.u., $B_C=B_{Lo}=1.0$ p.u.
$\alpha_{svco}=90^o$, $60^o\leq \alpha_{svc} \leq 135^o$, $K_s=1$, $T_s=0.05$ s., $|u_\alpha|=10$, $K_v=50$.
$K_{ps}=0.0683$, $K_{is}=8.0165$ and $K_{ds}=0.0483$.

Table 3 Conventional machines parameters

Unit	G_1	$G_{3, 4, 7}$	$G_{5, 8}$	G_6	G_9	G_{10}
Rated (MVA)	920.35	835	615	896	1070	410
X_d (p.u.)	1.7900	2.1830	0.8979	1.7900	1.933	1.7668
X'_d (p.u.)	0.3550	0.4130	0.2995	0.2200	0.4670	0.2738
X_q (p.u.)	1.6600	2.1570	0.6460	1.7150	1.7430	1.7469
X'_q (p.u.)	0.5700	1.2850	0.6460	0.4000	1.1440	1.0104
T'_{do} (s)	7.9000	5.6900	7.4000	4.3000	6.6600	5.4320
H (s)	3.7638	2.6424	5.148	2.9297	3.0953	3.7041
K_d (p.u.)	2.00	2.00	2.00	2.00	2.00	2.00

Table 3 Excitation systems and PSSs parameters

Unit	G_1	$G_{3, 4, 7}$	$G_{5, 8}$	G_6	G_9	G_{10}
K_A (p.u.)	25.000	400	200	250	400	400
T_A (s)	0.20	0.02	0.02	0.20	0.02	0.02
K_F (p.u.)	0.084	0.030	0.010	0.036	0.060	0.030
T_F (s)	1.00	1.00	1.00	1.00	1.00	1.00
E_{fdmax} (p.u.)	4.31	5.02	7.32	5.15	4.80	3.29
E_{fdmin} (p.u.)	-4.31	0.00	0.00	-5.15	0.00	0.00
G_S (p.u.)	0.03	0.03	0.03	0.03	0.03	0.03
T_1 (s)	0.15	0.15	0.15	0.15	0.15	0.15
T_2 (s)	0.015	0.015	0.015	0.015	0.015	0.015

STATCOM parameters

$G_s=1/28$ p.u.; $C_s=1$ p.u., $K_s=0.9$ p.u.
$K_{pc}=0.19024$, $K_{ic}=0.39253$, $K_{dc}=0.00207$
$K_{p\phi}=0.44093$, $K_{i\phi}=0.71248$, $K_{d\phi}=0.0063$
$K_{pv\phi}=0.71002$, $K_{iv\phi}=0.33503$
$K_{pvc}=0.39921$, $K_{ivc}=0.62223$

Appendix-B

SCG model

Based on Park's model used d-q axes transformation, the SCG nonlinear first-order differential equations are [14]:

I-Stator Representation:

$$\dot{\psi}_d = \omega_o (v_{td} + i_d R_a + \psi_q) + \omega\, \psi_q \quad (20)$$

$$\dot{\psi}_q = \omega_o (v_{tq} + i_q R_a - \psi_d) - \omega\, \psi_d \quad (21)$$

II-Outer Screen Representation:

$$\dot{\psi}_{D1} = -\omega_o\, i_{D1}\, R_{D1} \quad (22)$$

$$\dot{\psi}_{Q1} = -\omega_o\, i_{Q1}\, R_{Q1} \quad (23)$$

III-Inner Screen Representation:

$$\dot{\psi}_{D2} = -\omega_o\, i_{D2}\, R_{D2} \quad (24)$$

$$\dot{\psi}_{Q2} = -\omega_o\, i_{Q2}\, R_{Q2} \quad (25)$$

IV-Field Circuit Representation:

$$\dot{\psi}_f = \omega_o (v_f - i_f\, R_f) \quad (26)$$

The currents are obtained as a function of flux linkages as:

$$\begin{bmatrix} i_f \\ i_d \\ i_{D1} \\ i_{D2} \end{bmatrix} = \begin{bmatrix} X_f & -X_{fd} & X_{fD1} & X_{fD2} \\ X_{fd} & -X_d & X_{dD1} & X_{dD2} \\ X_{fD1} & -X_{dD1} & X_{D1} & X_{D1D2} \\ X_{fD2} & -X_{dD2} & X_{D1D2} & X_{D2} \end{bmatrix}^{-1} \begin{bmatrix} \psi_f \\ \psi_d \\ \psi_{D1} \\ \psi_{D2} \end{bmatrix} \quad (27)$$

and

$$\begin{bmatrix} i_q \\ i_{Q1} \\ i_{Q2} \end{bmatrix} = \begin{bmatrix} -X_q & X_{qQ1} & X_{qQ2} \\ -X_{qQ1} & X_{Q1} & X_{Q1Q2} \\ -X_{qQ2} & X_{Q1Q2} & X_{Q2} \end{bmatrix}^{-1} \begin{bmatrix} \psi_q \\ \psi_{Q1} \\ \psi_{Q2} \end{bmatrix} \quad (28)$$

V-Mechanical Equations:

$$\dot{\delta} = \omega \quad (29)$$

$$\dot{\omega} = \frac{\omega_o}{2H} (T_m - T_e) \quad (30)$$

where,

$$T_e = \psi_d i_q - \psi_q i_d \quad (31)$$

VI-Terminal power:

$$P_t = v_{td} i_d + v_{tq} i_q \quad (32)$$

VII-Terminal voltage:

$$v_t = \sqrt{v_{td}^2 + v_{tq}^2} \quad (33)$$

The model of the three stages steam turbine with reheat and electro-hydraulic governor is the IEEE standard representation as described in the model shown in Fig.21.

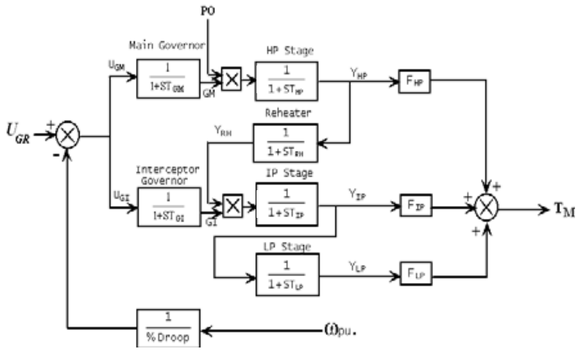

Fig.21 Representation of turbine and governor system

The mathematical model of the governor and turbine system is represented by a set of first order differential equations as:

I-The Electro-Hydraulic Governors Equations:

$$\dot{G}_M = \frac{U_{GM} - G_M}{T_{GM}} \quad (34)$$

$$\dot{G}_I = \frac{U_{GI} - G_I}{T_{GI}} \quad (35)$$

The valves travel and velocity limits are:
$0 \le G_M \le 1$, $-6.7 \le \dot{G}_M \le 6.7$ and $0 \le G_I \le 1$, $-6.7 \le \dot{G}_I \le 6.7$.

These rate change limits are based on the time required to reach the valves positions to 100% which is 150 ms [15].

II-Turbines Equations:

$$\dot{Y}_{HP} = \frac{G_M P_o - Y_{HP}}{T_{HP}} \quad (36)$$

$$\dot{Y}_{RH} = \frac{Y_{HP} - Y_{RH}}{T_{RH}} \quad (37)$$

$$\dot{Y}_{IP} = \frac{G_I Y_{RH} - Y_{IP}}{T_{IP}} \quad (38)$$

$$\dot{Y}_{LP} = \frac{Y_{IP} - Y_{LP}}{T_{LP}} \quad (39)$$

The mechanical torque is given by:

$$T_m = F_{HP} Y_{HP} + F_{IP} Y_{IP} + F_{LP} Y_{LP} \quad (40)$$

References:

[1] S. M. Osheba et al, “Comparison of transient performance of superconducting and conventional generators in a multimachine system”, IEE-Proc.135, pt. C, No. 5, Sept. 1988, pp.389-395.

[2] H. A. Khattab, “Stabilization of A Superconducting Generating Unit In A Multi-machine System”, Ph.D. Thesis, Menoufia University, Faculty of Engineering, 2007.

[3] G. A. Morsy, H. A. Kattab and A. Kinawy, “Design of a PI controller for a superconducting generator”, Eng. Research. Vol. 23, No. 1, Faculty of Engineering, Menoufiya, University, pp. 61-77, Jan. 2000.

[4] G. A. Morsy, T. A. Mohammed, “An ANN Based PI Controller For A Superconducting Generator”, Engineering Research. Vol. 24, No. 3, Faculty of Engineering, Menoufiya, University, pp. 113-125, June 2001.

[5] V. K. Sood, “HVDC and FACTS Controllers: Applications of Static Converters in Power Systems”, Kluwer, e- ISBN: 1-4020-7891-9, 2004.

[6] X. P. Zhang, C. Rehtanz and B. Pal, “Flexible AC Transmission Systems: Modelling and Control”, ISBN-10 3-540-30606-4, Springer-Verlag Berlin Heidelberg, 2006.

[7] E. Lerch et al, “Advanced SVC Control for Damping Power System Oscillations”, IEEE Transactions on Power Systems, Vol. 6, No. 2, pp 524-535, May 1991.

[8] F. Al-Jowder, “Improvement of Synchronizing Power and Damping Power by Means of SSSC and STATCOM: a Comparative Study”, Electric Power Systems Research, vol. 77, pp 1112–1117, 2007.

[9] K. R. Padiyar, “Design and Performance Evaluation of Subsynchronous Damping Controller With STATCOM”, IEEE Transactions on Power Delivery, vol. 21, No. 3, pp 1398-1405, July 2006.

[10] M.A. Pai, “Energy Function Analysis for Power System Stability”, Kluwer, 1989

[11] H. A. Khattab, “Control and Performance Analysis of A Superconducting Generator”, M.Sc. thesis, Menoufia University, Faculty of Engineering, 2000.

[12] R. A. Saleh, “Transient Voltage analysis and control of a superconducting Generator”, M.Sc.

thesis, Egypt, Menoufia University, Faculty of Engineering, 1993.
[13] E. Z. Zhou, “Application of static VAR Compensator to Increase Power System Damping”, IEEE Trans. on power systems, Vol. 8, No. 2, pp. 655-661,1993.
[14] R. A. Amer, “Artificial Intelligence Control for a Superconducting Generator in a Multimachine Power System”, M.Sc. thesis, Egypt, Menoufiya University, Faculty of Engineering, 2007.
[15] M. A. Alyan and Y. H. Rahim, “The role of governor control in transient stability of superconducting turbogenerators”, IEEE Trans.EC-2, March1987, pp.38-46.
[16] Yao-nan Yu, “Electric Power System Dynamics”, New York: Academic Press, 1983.
[17] L. Cong, Y. Wang and D.J. Hill, “Transient stability and voltage regulation enhancement via coordinated control of generator excitation and SVC”, Electrical Power and Energy Systems 27 (2005), pp.121-130.
[18] N.C. Sahooa et al, “Application of a multivariable feedback linearization scheme for STATCOM control”, Electric Power Systems Research, Vol. 62, Issue 2, 2002, pp 81-91.
[19] A. H .El-abiad, “Power systems analysis and planning”, Purdue University, West Lafayette, Indiana USA, 1983.
[20] S. M. Osheba , Y. H. A. Rahim, et al, “Stability of a Multi-Machine System Incorporating a Superconducting Alternator”, IEEE Trans. on Energy Conversion, Vol. 3, No.3, Sept.1988.
[21] G. A. Morsy, R. A. Amer, H. A. Yassin, “Unsupervised ANN Based PID Controller for a Superconducting Generator in a Multi-machine Power System”, Engineering Research Journal, Vol. 31, No. 1, January 2008, pp 23-32, Faculty of Engineering, Menoufiya University, Egypt.
[22] Q. Gu, A. Pandey and S. K. Starrett, “Fuzzy logic control schemes for static VAR compensator to control system damping using global signal”, Electric Power Systems Research 67 (2003), pp.115-122.